Homologs of the vancomycin resistance D-Ala–D-Ala dipeptidase VanX in *Streptomyces toyocaensis*, *Escherichia coli* and *Synechocystis*: attributes of catalytic efficiency, stereoselectivity and regulation with implications for function

Ivan AD Lessard[1], Steve D Pratt[2], Dewey G McCafferty[1]*, Dirksen E Bussiere[2], Charles Hutchins[2], Barry L Wanner[3], Leonard Katz[2] and Christopher T Walsh[1]

Background: Vancomycin-resistant enterococci are pathogenic bacteria that have altered cell-wall peptidoglycan termini (D-alanyl–D-lactate [D-Ala–D-lactate] instead of D-alanyl–D-alanine [D-Ala–D-Ala]), which results in a 1000-fold decreased affinity for binding vancomycin. The metallodipeptidase VanX (EntVanX) is a key enzyme in antibiotic resistance as it reduces the cellular pool of the D-Ala–D-Ala dipeptide.

Results: A bacterial genome search revealed *vanX* homologs in *Streptomyces toyocaensis* (StoVanX), *Escherichia coli* (EcoVanX), and *Synechocystis* sp. strain PCC6803 (SynVanX). Here, the D,D-dipeptidase catalytic activity of all three VanX homologs is validated, and the catalytic efficiencies and diastereoselectivity ratios for dipeptide cleavage are reported. The *ecovanX* gene is shown to have an RpoS (σ^s)-dependent promoter typical of genes turned on in stationary phase. Expression of *ecovanX* and an associated cluster of dipeptide permease genes permitted growth of *E. coli* using D-Ala–D-Ala as the sole carbon source.

Conclusions: The key residues of the EntVanX active site are strongly conserved in the VanX homologs, suggesting their active-site topologies are similar. StoVanX is a highly efficient D-Ala–D-Ala dipeptidase; its gene is located in a *vanHAX* operon, consistent with a vancomycin-immunity function. StoVanX is a potential source for the VanX found in gram-positive enterococci. The catalytic efficiencies of D-Ala–D-Ala hydrolysis for EcoVanX and SynVanX are 25-fold lower than for EntVanX, suggesting they have a role in cell-wall turnover. Clustered with the *ecovanX* gene is a putative dipeptide permease system that imports D-Ala–D-Ala into the cell. The combined action of EcoVanX and the permease could permit the use of D-Ala–D-Ala as a bacterial energy source under starvation conditions.

Addresses: [1]Department of Biological Chemistry and Molecular Pharmacology, Harvard Medical School, Boston, MA 02115, USA. [2]Pharmaceutical Products Division, Abbott Laboratories, Abbott Park, IL 60064, USA. [3]Department of Biological Sciences, Purdue University, West Lafayette, IN 47907, USA.

*Present address: Johnson Research Foundation and the Department of Biochemistry and Biophysics, University of Pennsylvania, Philadelphia, PA 19104, USA.

Correspondence: Christopher T Walsh
E-mail: walsh@walsh.med.harvard.edu

Key words: D-Ala-D-Ala dipeptidase, dipeptide permease, peptidoglycan recycling, RpoS-dependent genes, VanX

Received: **24 June 1998**
Accepted: **22 July 1998**

Published: **25 August 1998**

Chemistry & Biology September 1998, **5**:489–504
http://biomednet.com/elecref/1074552100500489

Introduction

Vancomycin-resistant enterococci (VRE) have become recognized as important opportunistic human pathogens over the past decade. As vancomycin has become a front-line drug for the treatment of enterococcal infections, as well as those caused by methicillin-resistant *Staphylococcus aureus* (MRSA), resistance and mortality from VRE has increased and an infectious catastrophe for MRSA is looming [1–4]. The most prevalent clinical phenotypes of vancomycin resistance, VanA and VanB [5], require expression of the genes *vanR*, *vanS*, *vanH*, *vanA*, and *vanX* (VanA phenotypic nomenclature) [6] to produce peptidoglycan chain precursors with altered termini for cell-wall biosynthesis that exhibit dramatically lower affinity for vancomycin. VanS and VanR act as a two-component regulatory system to mediate antibiotic-induced transcription of the genes *vanH*, *vanA*, and *vanX*, whose products act sequentially (VanH, VanA) to synthesize the depsipeptide D-alanyl–D-lactate (D-Ala–D-lactate), in place of the normal D-alanyl–D-alanine (D-Ala–D-Ala) dipeptide. VanX is a zinc-containing D,D-dipeptidase that hydrolyzes D-Ala–D-Ala but not D-Ala–D-lactate, allowing the D,D-depsipeptide to accumulate and become incorporated into the growing peptidoglycan termini. The modified peptidoglycan binds vancomycin 1000-fold less avidly than the D-Ala–D-Ala peptidoglycan [7,8] and results in unimpeded peptide-strand cross-linking, yielding a mechanically strong cell wall and resistance to lysis and cell death in the presence of vancomycin.

There is substantial interest in deciphering the mechanism, substrate selectivity and three-dimensional structure

Figure 1

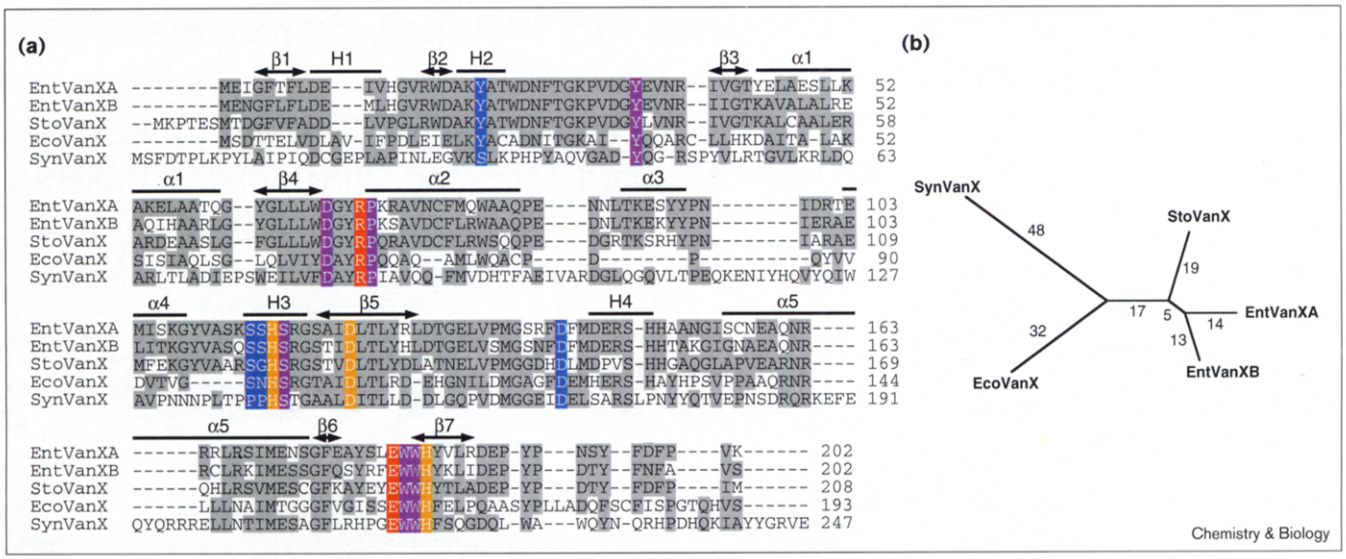

(a) Sequence alignment of the VanX homologs. EntVanXA, *Enterococcus faecium* VanX; EntVanXB, *E. faecalis* VanX; StoVanX, *Streptomyces toyocaensis* VanX homolog; EcoVanX, *Escherichia coli* VanX homolog; SynVanX, *Synechocystis* sp. PCC6803 VanX homolog. Identity and similarity are denoted by light gray background. The zinc ligands (orange), the catalytic base and transition-state residues (red), the substrate binding residues (blue) and the auxiliary residues involved in maintaining the active-site architecture (purple) are denoted by color boxes. The key portions of secondary structure of $EntVanX_A$ (α helices, β strands and 3_{10} helices) are denoted by their respective abbreviations; α, β and H. **(b)** Phylogenetic relationship among VanX homologs as calculated using the Clustal W method [52]. The branch length (numerical values in arbitrary units) is a measure of sequence divergence and is assumed to be approximately proportional to the phylogenetic distance. The phylogenetic tree was derived using the TREE program of Feng and Doolittle [59].

of VanX, given that metalloproteases operating in other biological contexts (e.g. angiotensin-converting enzyme) have been inhibited by rationally designed therapeutic agents (such as the angiotensin-converting-enzyme inhibitors). Among the relevant issues for investigation is the likely origin of the transposon-encoded *vanX* in VRE and its distribution in other bacteria, both gram-positive and gram-negative. We have recently reported a mutagenesis study on the *Enterococcus faecium* VanX (the $EntVanX_A$ from the VanA VRE phenotype), identifying putative enzyme ligands for zinc coordination and for general base catalysis of the attacking water molecule [9]. Crystallographic determination of the structure of $EntVanX_A$ has confirmed the conclusions of this study and revealed the enzyme architecture, including details of the active-site topology [10].

We have used the key residues in the zinc-binding motif of $EntVanX_A$ as a signature sequence to search for VanX homologs in bacterial genome databases to detect a VanX homolog from the glycopeptide-producer bacterial genome *Streptomyces toyocaensis* [11] and have found VanX type open reading frames (ORFs) in both gram-positive bacteria (*S. toyocaensis* [StoVanX], 64% similarity with $EntVanX_A$) and, with much lower homology, in gram-negative bacteria (*Escherichia coli* [EcoVanX], 27% similarity; *Synechocystis* sp. strain PCC6803 [SynVanX], 16% similarity). We report here the purification and validation of enzymatic zinc-dependent D,D-dipeptidase activity of these three bacterial VanX homologs. Furthermore, we have analyzed the potential functions of EcoVanX and five downstream genes for catabolic function, induced during stationary phase by the σ^s factor of *E. coli* RNA polymerase.

Results

Residues that predict zinc-dependent D,D-dipeptidase activity

In an earlier study of the zinc-dependent metallodipeptidase $EntVanX_A$ required for clinically significant vancomycin resistance, we identified, using site-directed mutagenesis, residues His116, Asp123 and His184 as likely ligands for zinc coordination and Glu181 as the probable general base for deprotonation of the zinc-coordinated water molecule that subsequently attacks the D-Ala–D-Ala substrate [9]. The recent crystallographic structure determination of $EntVanX_A$ has borne out these assignments [10] and has led us to search for homologs of VanX in other bacterial genomes to gain insight into the structural and functional origins of the transposon-borne EntVanX. As illustrated in Figure 1a, the zinc ligand and general base residues are conserved in the similarly sized StoVanX (208 amino acids [aa]), EcoVanX (193 aa) and SynVanX (247 aa) ORFs, suggesting that they are *bona fide* members of the zinc-protease VanX family, even though the low

Figure 2

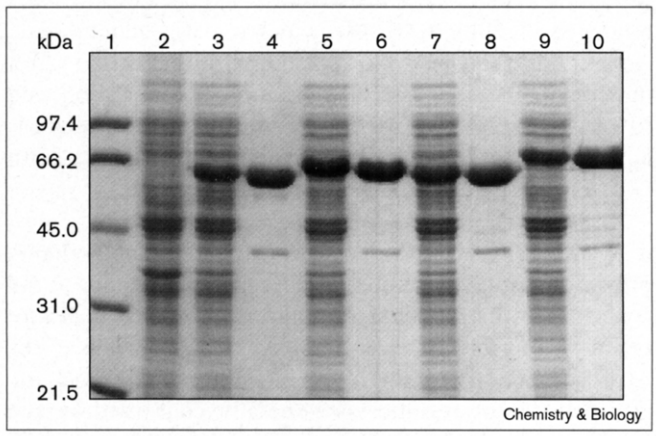

Overproduction and purification of MBP–VanX fusion proteins. *E. coli* BL21(DE3) cells were transformed with pIADL14/pIADL55/pIADL58 or pIADL61, grown, and induced with IPTG as described in the Materials and methods section. Each recombinant MBP–VanX fusion protein was purified on an amylose column. Protein samples were analyzed for purity using SDS–PAGE with Coomassie Blue staining. Lane 1, molecular weight markers (phosphorylase B, 97.4 kDa; serum albumin, 66.2 kDa; ovalbumin, 45.0 kDa; carbonic anhydrase, 31.0 kDa; trypsin inhibitor, 21.5 kDa; lysozyme, 14.4 kDa); lane 2, *E. coli* cells transformed with pIADL14 (before induction); lanes 3, 5, 7 and 9, clarified lysate of induced cells transformed with pIADL14, pIADL61, pIADL55 and pIADL58 respectively; lanes 4, 6, 8 and 10, MBP fusion protein eluted from the amylose column (MBP–EntVanX, MBP–StoVanX, MBP–EcoVanX and MBP–SynVanX, respectively).

Table 1

Kinetic parameters and zinc content of purified MBP–VanX fusion proteins.

Substrate	Protein	k_{cat}(s^{-1})	K_M(μM)	k_{cat}/K_M (s^{-1} mM^{-1})	mol % Zn content
D-Ala–D-Ala	EntVanX	26	80	325	95
	StoVanX	12	4.0	3000	84
	EcoVanX	170	1.4×10^3	12	100
	SynVanX	310	1.6×10^3	19	55
L-Ala–D-Ala	EntVanX	1.2	30×10^3	0.04	
	StoVanX	10	6.8×10^3	1.5	
	EcoVanX	70	$> 550 \times 10^3$	0.13	
	SynVanX	110	8.3×10^3	13	

sequence similarity of 27% for EcoVanX and 16% for SynVanX might have otherwise been below detection limits (Figure 1b). To overproduce the three VanX homologs in *Escherichia coli*, the affinity purification strategy used for $EntVanX_A$ (202 aa) involving in-frame fusions to maltose-binding protein (MBP) was adapted, and led to single-step purification of each of the three $EntVanX_A$ homologs (Figure 2). Zinc analysis revealed that all the VanX homologs did contain the metal ion, although the SynVanX protein contained only 55 mol% zinc (Table 1). We have not attempted additional quantitation of the zinc content of SynVanX, but have used the result as a validation of the anticipated zinc-dependent dipeptidase activity of this enzyme. In keeping with this prediction, and as observed with $EntVanX_A$ [9], all the VanX homologs retained activity as D,D-dipeptidases when fused to MBP. Thus, the kinetic data reported in Table 1 were obtained using the intact MBP-fusion protein in each case.

Catalytic properties of VanX homologs

Table 1 reveals a one log variation in k_{cat} for D-Ala–D-Ala hydrolysis by the various VanX homologs (12 s^{-1} for StoVanX; 310 s^{-1} for SynVanX). The variation in K_M values was much larger (4 μM for StoVanX; 14 mM and 16 mM for EcoVanX and SynVanX respectively). Correspondingly, the catalytic efficiency (k_{cat}/K_M) of StoVanX (3,000 $mM^{-1}s^{-1}$) is tenfold better than that of $EntVanX_A$ (325 $mM^{-1}s^{-1}$) and 150- and 250-fold higher than that of SynVanX and EcoVanX, respectively.

The 4,000-fold variation in K_M values for D-Ala–D-Ala observed in the VanX homologs prompted a search for alternate substrates of these enzymes, especially for EcoVanX and SynVanX, which have high K_M values. No dipeptidase activity was detected with L-Ala–L-Ala or D-Ala–L-Ala for any of the four enzymes, but the heterochiral dipeptide L-Ala–D-Ala was accepted as substrate (see below; Table 2). As observed with $EntVanX_A$ [12], both the N^{α}-amino group and the carboxylate moiety of the dipeptide substrate had to be free as evidenced by the absence of peptidase activity towards *N*-acetyl-D-Ala–D-Ala and D-Ala–D-Ala-*O*-methyl ester (Table 2). Discrimination between the peptide-bond cleavage (D-Ala–D-Ala) and the analogous ester-bond cleavage (D-Ala–D-lactate) reported for $EntVanX_A$, is also observed for all three VanX homologs (Table 2).

The L-Ala–D-Ala hydrolase activity data for the VanX homologs are summarized in Table 1. The k_{cat} values for turnover were respectable, ranging from 1.2 s^{-1} ($EntVanX_A$) to 110 s^{-1} (SynVanX). The K_M values for the L,D-dipeptide are generally much higher that those for the cognate D,D-substrate. For example, StoVanX recognizes L-Ala–D-Ala with a K_M of 6.8 mM, which is 1,700-fold worse than its affinity for D-Ala–D-Ala (K_M of 4 μM). Similarly, $EntVanX_A$ recognizes the L,D-dipeptide 400-fold worse than the D,D-dipeptide substrates. Because EcoVanX activity was not saturated, even at 300 mM L,D-dipeptide, a K_M greater than 550 mM is estimated for this substrate. In sharp contrast, SynVanX has a twofold lower K_M for the L,D-dipeptide (8.3 mM) versus the D,D-dipeptide (16 mM). The ratios of catalytic efficiency (k_{cat}/K_M) for L-Ala–D-Ala and D-Ala–D-Ala are 10^{-5}:1 to 10^{-4}:1 for $EntVanX_A$ and StoVanX, respectively, and emphasize this discrimination. EcoVanX shows a 10^{-2}:1 ratio, whereas SynVanX is clearly indifferent to

Table 2

Substrate specificity of the various VanX homologs as dipeptidases and oligopeptidases.

Substrate	EntVanX	StoVanX	EcoVanX	SynVanX
D-Ala–D-Ala	+	+	+	+
D-Ala–L-Ala	–	–	–	–
L-Ala–D-Ala	+	+	+	+
L-Ala–L-Ala	–	–	–	–
Aib–D-Ala*	+	+	+	+
L-Ala–D-GluNH$_2$	–	–	–	–
D-Ala–D-Ala-OMe	–	–	–	–
*N*Ac-D-Ala–D-Ala	–	–	–	–
D-Ala–D-Ala–D-Ala	–	–	–	–
L-Ala–L-Ala–L-Ala	–	–	–	–
D-Ala–D-lactate	–	–	–	–
D-Ala–γ-D-Glu–L-Lys–D-Ala–D-Ala	–	–	–	–

Each substrate (10 mM) was incubated with 2–4 μM enzyme and the activity was determined visually by the Cd-ninhydrin assay (see the Materials and methods section). *Aminoisobutyryl–D-Ala.

the chirality of the first alanine residue, with a ratio of 0.7:1. This last result predicted that SynVanX should process the dipeptide aminoisobutyryl–D-Ala efficiently, consistent with its ability to accommodate the methyl sidechain of both D-Ala and L-Ala. Only a low dipeptidase activity could be detected with this substrate, however, indicating that either structurally hindered molecules were not tolerated or that conformational constraints of the α,α-dialkyl residue prevented hydrolysis of the peptide bond (data not shown).

Sequence and structural homology of VanX homologs with EntVanX$_A$

The recent crystallographic determination of the structure of EntVanX$_A$ protein has revealed several key residues involved in binding and cleavage of the D-Ala–D-Ala substrate, and in maintaining the active-site structure [10]. These residues can be categorized as follows: zinc ligands (His116, Asp123 and His184), catalytic residues (Glu181 and Arg71), substrate-binding residues (Tyr21, Asp123, Asp142, Ser114 and Ser115), and auxiliary residues at the active site (Tyr35, Asp68, Pro72, Ser117, Trp182 and Trp183). As illustrated in Figure 1a, despite the low percentage of overall sequence similarity between EntVanX$_A$ and EcoVanX (27%) or SynVanX (16%), the key active-site residues are conserved, which implies, together with the dipeptidase activity, that these enzymes use similar mechanisms for proteolysis and substrate binding, and confirms a functional role for these homologs as zinc-dependent D,D-dipeptidases.

For all VanX homologs, the three residues involved in zinc coordination (His116, Asp123 and His184) are conserved, consistent with the presence of zinc in the purified enzymes (Table 1). In EntVanX$_A$, the nucleophilicity of a water molecule, the fourth zinc ligand, is enhanced by hydrogen bonding to Glu181, which acts as a general base. Attack of the scissile peptide bond by this activated water molecule generates a tetrahedral adduct that is believed to be stabilized by Arg71. This mechanism of catalysis appears to operate in all the VanX homologs, as both Glu181 and Arg71 are conserved in each system.

The active site of EntVanX$_A$ is capable of accommodating only a dipeptide as a substrate because it is compact and consists of a narrow channel lined at the distal end with residues (Tyr21, Asp123 and Asp142) that make key hydrogen bonds with the N^{α}-amino group of the substrate. This cluster of residues is generally conserved in the VanX homologs, although a serine residue (which can still participate in hydrogen bonding) replaces Tyr21 of EntVanX$_A$ in SynVanX. Such an active-site topology emphasizes the prerequisite for a free primary amino group in the substrate and would explain the absence of activity towards protected-amino-group substrates for all VanX homologs (Table 2). A significant diversity in residue identity is observed at positions corresponding to Ser114 and Ser115 in EntVanX$_A$, believed to be involved in binding of the carboxylate group of the D-Ala–D-Ala substrate [10]. Ser114 is conserved in two homologs but a proline residue is found at this position in SynVanX. Ser115 is absent in all homologs, including the tenfold more efficient enzyme StoVanX. Substitution of Ser115 with bulkier residues (asparagine in EcoVanX and proline in SynVanX) could account for the higher K_M values for D-Ala–D-Ala observed in these systems.

Striking similarities are found in the auxiliary residues that maintain the active-site topology in the VanX family of proteins. In EntVanX$_A$, Asp68 is positioned to form hydrogen bonds with Tyr35 and the ε-nitrogen of Arg71, which is believed to be important in ensuring the proper orientation of Arg71 in the active site. These residues, which comprise the hydrogen-bonding triads, are conserved in all VanX homologs. Similarly, Ser117 in EntVanX$_A$ hydrogen bonds with Pro72, which, in turn, hydrogen bonds to His116, thereby assuring the proper orientation of His116. Again, these residues are conserved in all the VanX homologs. The conserved residues Trp182 and Trp183 appear to be involved in enzyme stability. Trp182 forms an aromatic network with several other aromatic sidechains, namely Trp67, Phe141 and Tyr21. As is typical of such interactions, the aromatic groups lie in a herringbone pattern [13]. It should be noted that the aromatic character of these residues is highly conserved across the identified VanX homologs. There is also the possibility of Trp183 acting as a hydrogen-bond acceptor for the amino-group of the first residue of the D-Ala–D-Ala substrate, as is shown in the co-crystal structure of EntVanX$_A$ with D-Ala–D-Ala [10].

The hydrogen-bond distance of 3.8 Å suggests this is a weak bond (if it does exist).

Three-dimensional homology modeling of EcoVanX

The conservation of key active-site residues in the VanX homologs together with the modest overall sequence homology allowed homology modeling of the three-dimensional structure of a typical EntVanX homolog (EcoVanX; Figure 1a) using the crystal structure of EntVanX$_A$ as structural template. The alignment and model follow the rules of protein folding: residues are in suitable chemical and structural environments. Insertion and deletions within the *E. coli* homolog occur primarily outside elements of secondary structure with the exception of a small deletion in the α2 helix and the deletion of the entire α3 helix; the loop between the α4 and H3 helices is also absent. The resulting homology model superimposes with the crystal structure with an RMS deviation of 1.38 Å over 176 α-carbons (Figure 3a). Major alterations are seen in the mainchain path at the carboxyl terminus where several small 2–3 residue insertions have occurred. Despite these modifications, the active site remains virtually identical to that of EntVanX$_A$ (Figure 3b). The residues responsible for zinc coordination are present, represented by His98, Asp105, and His165. The key catalytic residues, Arg71 and Glu162, are also present, as are the residues responsible for interacting with the amino group of the substrate (Tyr23, Asp123, and Asp105). Residues responsible for interacting with the carboxylate of the substrate (Ser96 and Asn97) are shifted inwards towards the active site by 2–3 Å; this alteration is due to a deletion amino-terminal to this portion of the molecule. The repositioning of this loop might be one of the factors for the increased K_M observed for D-Ala–D-Ala. Another contributor to the increased K_M is most certainly the minor repositioning of key sidechains, which cannot be predicted by the model. Aside from the noted differences, the differences between the crystal structure and the homology model are negligible. The structural and sequence conservation between VanX homologs suggests this to be a case of divergent evolution wherein all the homologs are derived from a common ancestor. This hypothesis is strengthened by the sequence comparison, where the most divergence is seen within loops and the highest identity is seen within key catalytic-residue positions and domains of secondary structure.

Possible physiological roles for EcoVanX

Analysis of the gene organization at minute 33.7 of the *E. coli* chromosome (Figure 4), reveals that *ecovanX* is directly (13 basepairs [bp]) upstream of five ORFs with homology to oligopeptide and dipeptide permease genes. The latter genes also are organized in a fashion similar to other peptide permease clusters, and would be sufficient to code for a complete transport system with periplasmic and membrane components. Noteworthy is the *orfA* (f516) gene

Figure 3

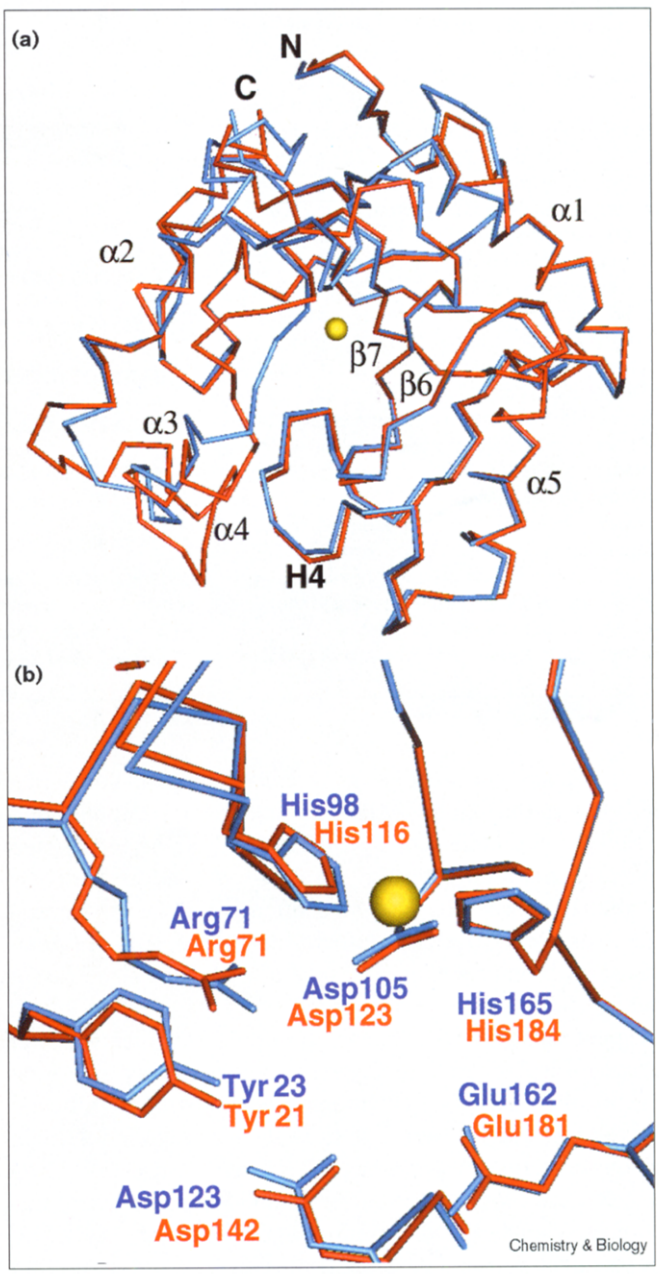

Comparison of the EcoVanX structural homology model (red) with EntVanX$_A$ (blue). **(a)** Comparison of the α-carbon backbone. **(b)** Comparison of the key active-site residues (numbering, EntVanX$_A$ [EcoVanX]): zinc ligands (His116 [His98], His184 [His165] and Asp123 [Asp105]), catalytic residues (Glu181 [Glu162] and Arg71 [Arg71]) and substrate binding (N^{α}-amino group; Tyr21 [Tyr23] and Aps142 [Asp123]). The zinc ion is shown as a yellow sphere.

(Figure 4), which codes for a homolog to the periplasmic dipeptide-binding protein DppA in *E. coli* (23% similarity) [14]. If D,D- (or L,D-) dipeptides are thereby imported, perhaps cytoplasmic EcoVanX catabolizes such dipeptide metabolites. Coexpression of *ecovanX* and the permease gene cluster is demonstrated below.

Figure 4

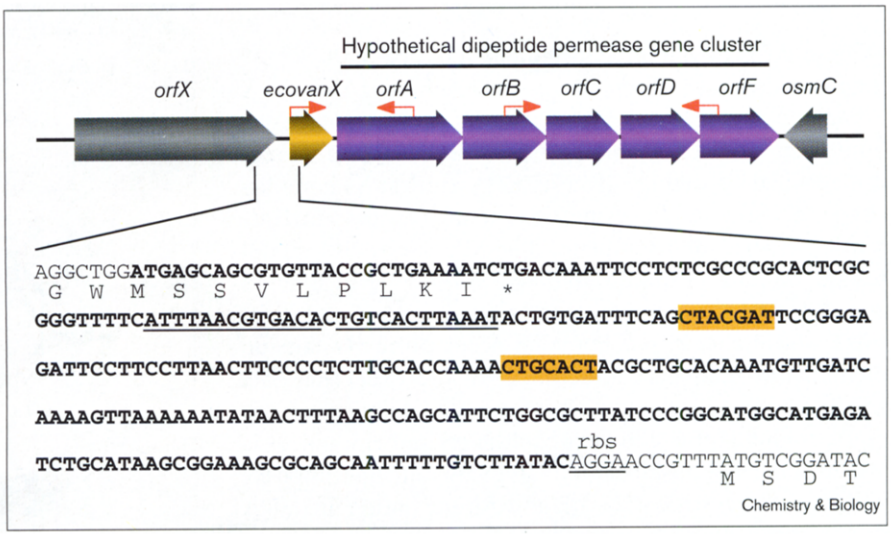

Gene organization at 33.7 minutes of the *E. coli* chromosome [45]. *ecovanX*, EcoVanX gene product (ORF-f193, accession 1787763); *orfA*, gene coding for a homolog to the dipeptide-binding protein DppA from *E. coli* (ORF-f516, accession 1787762); *orfB*, gene coding for a homolog to the dipeptide transport permease DppB from *E. coli* (ORF-f340, accession 1787761); *orfC*, gene coding for a homolog to the dipeptide transport permease DppC from *E. coli* (ORF-f298, accession 1787760); *orfD*, gene coding for a homolog to the oligopeptide transport ATP-binding protein OppD from *Salmonella thyphimurium* (ORF-f328, accession 1787759); *orfF*, gene coding for a homolog to the oligopeptide transport ATP-binding protein AppF from *Bacillus subtillis* (ORF-f308, accession 1787758); *orfX*, hypothetical protein gene product (ORF-f807, accession 1787765); *osmC*, gene for osmotically inducible protein. The noncoding sequence between the *orfX* gene and the *ecovanX* gene is shown. A putative transcriptional terminator for the *orfX* gene and the ribosome binding site (rbs) for the *ecovanX* gene is underlined. The putative σ^s −10 regions are indicated by orange boxes. The region used for a transcriptional fusion construct with *lacZ* (see Figure 5a) is indicated in bold. The red arrows indicate the sites of priming sites used for the RT–PCR (see Figure 5b).

Upstream of the *ecovanX* gene are ~260 bp of noncoding DNA with two putative −10 sequences for a σ^s (RpoS) regulated promoter (consensus: CTATACT [15]; Figure 4), suggesting that this cluster of genes is induced during stationary phase [16]. A −10 sequence for the σ^{70}-dependent promoter was also detected in this region; the putative −35 promoter sequence is at a spacing so close that it would be placed on the opposite face of the DNA with respect to the −10 element, however. To test whether *ecovanX* is indeed regulated by the stationary phase σ^s factor of *E. coli* RNA polymerase, we constructed a fusion of the proposed promoter with *lacZ* and integrated a single copy into the chromosome of *E. coli* strains BW22653 (*rpoS*$^+$) and BW24180 (*rpoS*$^-$) to establish whether there was a dependence on σ^s (strains IALD310 and IADL313, respectively). Indeed, growth studies showed a tenfold induction of the $P_{ecovanX}$–*lacZ* fusion only in the strain carrying a functional *rpoS* gene (Figure 5a). Induction is activated early during the transition into stationary phase as observed in other σ^s-dependent genes (e.g., *otsAB* [17] and *bolA* [18]). The phenotype of σ^s-dependent induction could be restored in the *rpoS* mutant strain by the presence of plasmid pDEB2 expressing the *rpoS* gene (data not shown).

We have used reverse transcription polymerase chain reaction (RT–PCR) technology to determine if *ecovanX* and the dipeptide permease genes are coexpressed during stationary phase. Although we were not able to find conditions for an RT–PCR product of the entire cluster (expected product of over 6,000 bp), we were able to RT-PCR amplify the region that includes the *ecovanX* gene and the first gene of the putative dipeptide permease cluster (*orfA*). (Figure 5b (i), Figure 4). In a separate reaction we also detected an RT–PCR product corresponding to the distal four genes (*orfBCDF*) of the dipeptide permease cluster (Figure 5b (ii), Figure 4). Furthermore, both products showed a similar pattern of transcription, with the highest level during stationary phase, in agreement with the transcriptional fusion study of the $P_{ecovanX}$ with *lacZ* (see above and Figure 5a). These results show that the *ecovanX* and the dipeptide permease genes form a tight cluster that is induced during stationary phase.

Growth of *E. coli* on D-Ala–D-Ala as carbon and energy source

Initial attempts to detect growth of *E. coli* BW25113 on D-Ala–D-Ala were not successful although, *E. coli* has been reported to grow on D-Ala [19]. If sufficient EcoVanX were produced, one would expect growth by subsequent oxidation of the D-Ala by the membrane bound D-amino acid dehydrogenase (D-ADH), which passes electrons into the respiratory chain [20]. In the event that the level of expression of *ecovanX* was too low to sustain growth under laboratory conditions, we constructed an *E. coli* strain (IADL307) harboring a second copy of the *ecovanX* gene under the control of P_{lac} to induce high level expression. In fact, this strain showed growth on D-Ala–D-Ala, whereas the parent strain (BW25113), which has the resident *ecovanX* gene under its own promoter, did not sustain growth (Figure 6). The growth of strain IADL307 was also sustained in the absence of the inducer IPTG, suggesting that low levels

Figure 5

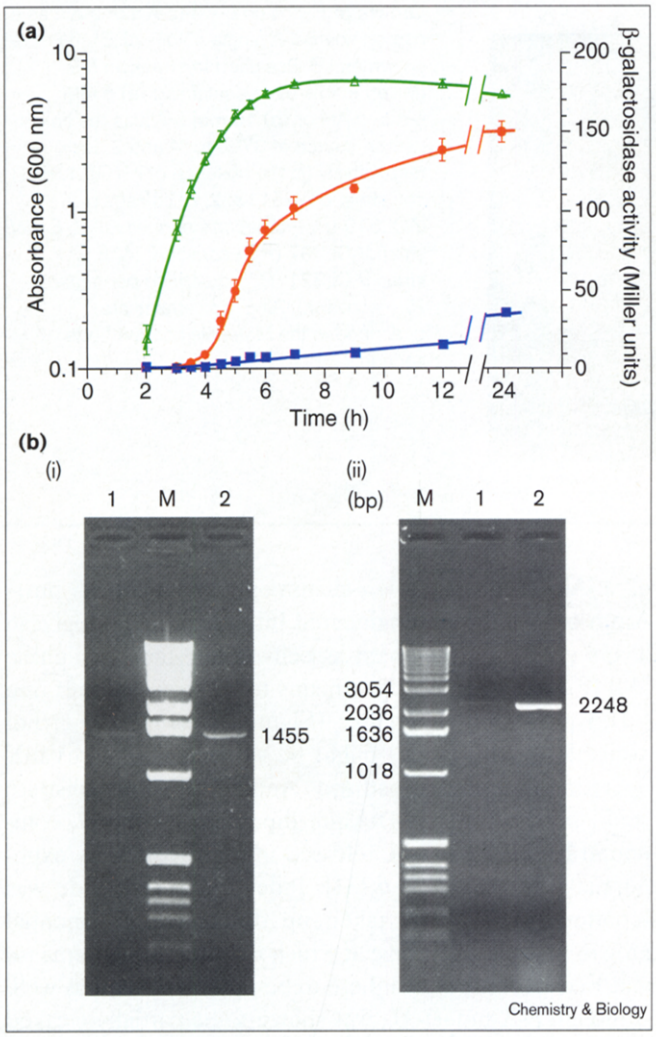

(a) Involvement of *rpoS* in a growth-phase-dependent induction of *lacZ* by the *ecovanX* promoter (see Figure 4). Expression of *lacZ* was determined in isogenic *rpoS*$^+$ (red circles) and *rpoS*$^-$ (blue squares) strains. Stationary phase cultures were diluted (1:10) into LB medium and incubated at 37°C with agitation for 30 min. The dilution and incubation steps were repeated three times. The growth at 37°C was monitored by absorbance at 600 nm (green triangles, average of all cultures) and specific β-galactosidase activity (Miller units) was determined at various growth stages. These experiments were carried out in triplicate. **(b)** Analysis of the *ecovanX* and dipeptide permease transcripts. Total RNA was prepared from *E. coli* NM522 cultures in exponential phase (lane 1) and stationary phase (lane 2) and was used to amplify the gene cluster by RT–PCR (see Figure 4) as described in the Materials and methods section. (i) shows the PCR product of the region from *ecovanX* to *orfA* (expected 1455 bp). (ii) shows the PCR product of the region from *orfB* to *orfF* (expected 2248 bp). Identity of the PCR products was confirmed by restriction mapping (data not shown).

of expression were sufficient (P_{lac} is repressed by LacI^q present in these strains).

Previously we observed that overproduction of EntVanX$_A$ under control of the T7 promoter in *E. coli* led to rapid cell death and lysis [9], in contrast to the successful overproduction of EcoVanX from the same promoter (this work). To assess whether cell death was due to the higher catalytic efficiency of EntVanX$_A$ as a D-Ala–D-Ala hydrolase, an *E. coli* strain (IADL318) harboring a single chromosomal copy of the *entvanX*$_A$ gene under P_{lac} control was made. Indeed this strain shows growth on D-Ala–D-Ala (data not shown), suggesting that there is a fine balance between sufficient dipeptidase activity to sustain growth, and so much enzyme that all intracellular D-Ala–D-Ala is hydrolyzed and cell-wall synthesis is halted.

Discussion

Of the five resistance proteins, VanR, VanS, VanA, VanH and VanX in VanA and VanB phenotypes of vancomycin-resistant enterococci (VRE), VanX was the only one for which homology searches did not initially reveal function by relationship to other known proteins [6,21–23]. The first indication that VanX functions as a D,D-dipeptidase came from the work of Reynolds *et al.* [7]; it was only after detection of zinc in the purified EntVanX$_A$ enzyme [12] and subsequent identification of putative zinc-ligand residues by site-directed mutagenesis [9] that the connection to the D,D-carboxypeptidases VanY [24,25], the *Streptomyces albus G* D-Ala–D-Ala carboxypeptidase [26] and to some phage-encoded endolysins [9] was discovered. The function of EntVanX is clearly to alter the pools of cytoplasmic D-Ala–D-lactate:D-Ala–D-Ala by selective hydrolytic removal (10^{-6}:1) of the dipeptide [12], such that D-Ala–D-lactate is preferentially utilized in enterococcal cell-wall biosynthesis, yielding essentially all nascent peptidoglycan chains terminating in D-Ala–D-lactate, enabling vancomycin resistance. The basis of the million-fold preference for D,D-dipeptide as substrate for VanX instead of D,D-depsipeptide is not yet understood in EntVanX or any of the VanX homologs.

The recent detection of a *vanHAX* gene cluster in the glycopeptide-antibiotic-producing *S. toyocaensis* [11], and the demonstration herein that purified StoVanX possesses both the anticipated D-Ala–D-Ala dipeptidase activity and lacks D-Ala–D-lactate depsipeptidase activity is satisfying on several accounts. First, it suggests a clear and conserved mechanism for the observed intrinsic resistance of the antibiotic producers to the vancomycin class of glycopeptides. Second, it suggests an obvious evolutionary source of the genes encoding VanHAX proteins (54%, 63%, 64% homology, respectively, to the EntVanHAX counterpart in the VanA phenotype) in pathogenic VRE, by gene transfer from such antibiotic producers, and is consistent with the view that antibiotic resistance genes might have evolved at the same time as antibiotic biosynthesis genes. In *S. toyocaensis* there are two D-,D-ligases: a D-Ala–D-Ala ligase and a D-Ala–D-lactate ligase [27]; the latter could be switched on transcriptionally as the host commences antibiotic biosynthesis, allowing cell-wall termini

Figure 6

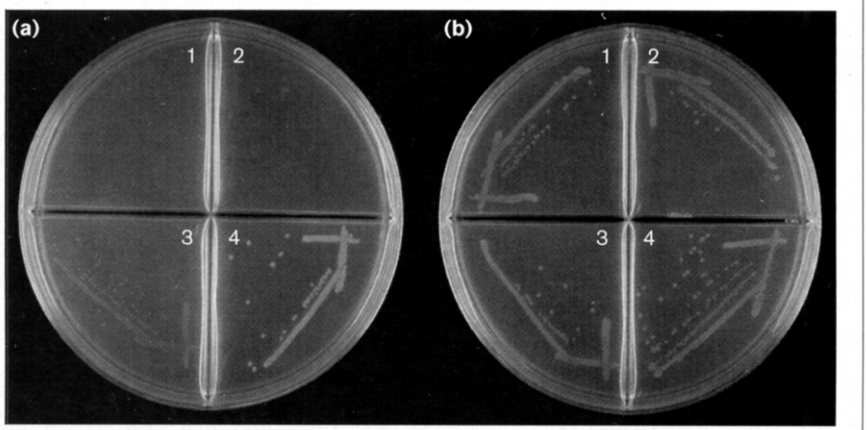

Growth of *E. coli* on D-Ala–D-Ala or D-Ala as a carbon source. A single colony of *E. coli* grown on LB was used to streak an M9 (Miller) media plate containing **(a)** 5 mM D-Ala–D-Ala or **(b)** 10 mM D-Ala as the sole carbon source at 37°C for 4 and 2 days, respectively (in the absence of IPTG). 1, *E. coli* strain BW25113; 2, *E. coli* strain IADL319 (P_{lac}–*dipeptide permease*); 3, *E. coli* strain IADL307 (P_{lac}–*ecovanX*); 4, *E. coli* strain IADL321 (P_{lac}–*dipeptide permease*, P_{lac}–*ecovanX*). All *E. coli* strains are described in the Materials and methods section.

to be reprogrammed to create immunity to vancomycin in a timely fashion. Such a regulatory circuit has yet to be verified experimentally.

It is highly likely that EntVanX and StoVanX serve analogous functions in the physiological destruction of D-Ala–D-Ala in the cytoplasm and the high k_{cat}/K_M catalytic efficiency ratios of 3.25×10^5 $M^{-1}s^{-1}$ and 3×10^6 $M^{-1}s^{-1}$ for dipeptide hydrolysis are consistent with this prediction. In contrast, EcoVanX and SynVanX fall short in catalytic efficiency (20-fold less effective), with a 200-fold increase in K_M values for D-Ala–D-Ala for these enzymes compared to $EntVanX_A$. The relative inefficiency of these two VanX homologs in binding and hydrolysis of D,D-dipeptides tempered our initial surprise upon discovering these proteins in the cyanobacterium *Synechocystis* and in particular in *E. coli*. There is no comparable D-Ala–D-lactate peptidoglycan alternative pathway for cell-wall biosynthesis in *E. coli* and, as gram-negative organisms, *Synechocystis* and *E. coli* are never challenged by glycopeptide antibiotics of the vancomycin class (because the antibiotic cannot penetrate the outer cell membrane).

The above observations raised the prospect that the EcoVanX homolog, which clearly possesses zinc D,D-dipeptidase activity, might operate on an alternate substrate, derived from the peptidoglycan layer (Figure 7). For example, one could imagine murein hydrolase roles for this enzyme. In this regard, D,D-endopeptidase, D,D-carboxypeptidase, and L,D-carboxypeptidase activities have been previously described for *E. coli* [28,29]. The initial scan of potential peptidyl substrates (Table 2) rules against hydrolysis of *N*-acyl-D-Ala–D-Ala and oligopeptides (no D(L),D(L)-carboxypeptidase or D(L),D(L)-endopeptidase activity in EcoVanX) but L,D-dipeptidase activity is possible. Although the catalytic efficiency for L-Ala–D-Ala is unimpressive and there is no known physiological source of L-Ala–D-Ala, L,D-*meso*-diaminopimelic acid (A_2pm)–A_2pm cross-links are engineered into *E. coli* peptidoglycan layers (10% of cross-links) as cells enter stationary phase [30] (Figure 7 and 8b). It remains to be seen whether free L,D-A_2pm–A_2pm dipeptides (Figure 7, compound c; not available for this study) might be substrates for EcoVanX operating in a salvage pathway. Another possible substrate could be the L-A_2pm–D-A_2pm dipeptide (Figure 7, compound b) reported to be released in the medium by exponentially growing *E. coli* [31]. Indeed, this dipeptide was reported to be poorly taken up during the exponential growth phase [32], a stage at which the dipeptide permease and EcoVanX are shown here to be poorly induced as well. Although L-A_2pm–D-Ala was shown to be partially cleaved before uptake [32], the sequential activity of the dipeptide permease and EcoVanX could represent a salvage pathway for this pseudopeptide during stationary phase. An L-A_2pm–D-Ala (L-Lys–D-Ala) dipeptidase enzyme has been characterized in sporulating cells of *Bacillus sphaericus* 9602 [33]. Contrary to EcoVanX, this enzyme showed no activity on D-Ala–D-Ala. There is no known L,D-endopeptidase that could cleave the peptidogycan linkage L-Ala–D-Glu, but cleavage of the linkage between D-Glu–L-A_2pm has been described in organisms other than *E. coli* [34]. Although not explicitly detected, L-Ala–D-Glu and D-Glu–L-A_2pm dipeptides are potential fragments of peptidogycan turnover (Figure 7, compounds a and f, respectively). An L-Ala–D-GluNH_2 dipeptide did not show any activity with purified EcoVanX and because of the strict exclusion of L-amino acid at the carboxyl terminus of the dipeptide, the dipeptide D-Glu–L-A_2pm is also unlikely to be an EcoVanX substrate.

A more likely scenario is that D-Ala–D-Ala is the physiological substrate for EcoVanX, in which case its regulation must be tightly controlled as there can be few circumstances under which *E. coli* will hydrolyze substantial

Figure 7

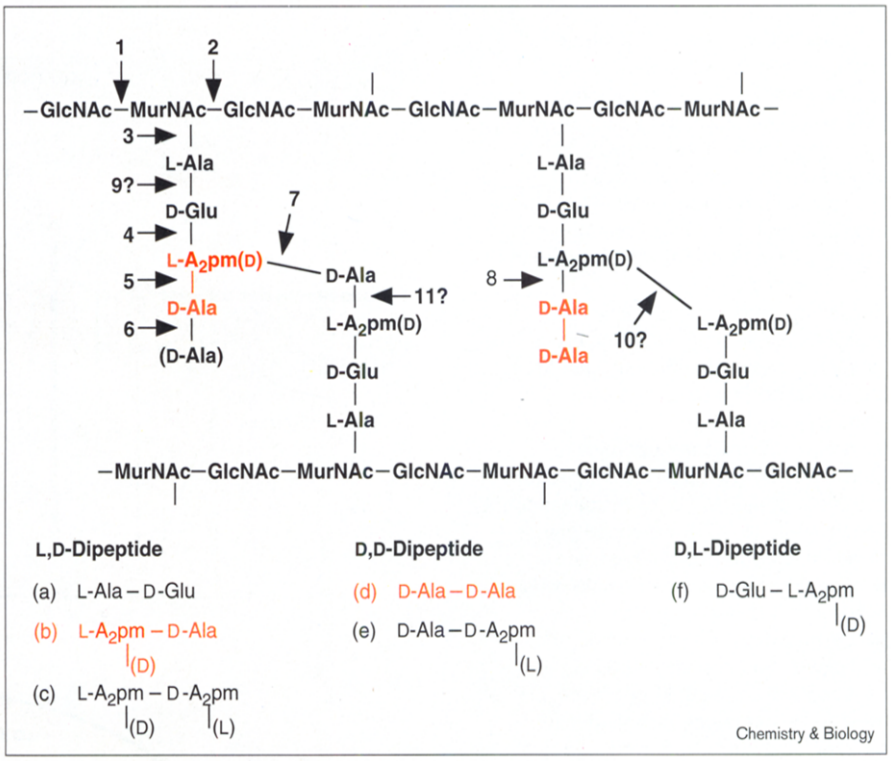

Possible dipeptides from endopeptidase, muramidase and carboxypeptidase action on *E. coli* peptidoglycan. D-Ala–D-A_2pm is the prevailing cross-link [37]. During stationary phase, A_2pm–A_2pm cross-linkages increase up to 10% of total cross-linkages [31]. Cleavage between L-Ala–D-Glu has not been discovered (**9**) nor between A_2pm–A_2pm (**10**). The formation of the dipeptide D-Ala–D-A_2pm requires the action of a putative L-A_2pm–D-Ala endopeptidase (**11**). In red are dipeptide products identified to be released by *E. coli* [32,38]. The numbers indicate the cleavage point by a specific murein hydrolase: **1**, *N*-acetylglucosaminidase; **2**, lytic transglycolase; **3**, *N*-acetylmuramyl-L-alanine amidase; **4**, γ-D-glutamyl-L-diaminopimelic acid endopeptidase; **5**, L,D-carboxypeptidase; **6**, D,D-carboxypeptidase; **7**, D,D-endopeptidase; **8**, L,D-dipeptidylcarboxypeptidase. A_2pm, diaminopimelic acid; GlcNAc, *N*-acetylglucosamine; MurNAc, *N*-acetylmuramic acid.

amounts of its D-Ala–D-Ala cytoplasmic pool and put peptidoglycan synthesis at risk (we suggest below that the source of D-Ala–D-Ala for EcovanX action might in fact be periplasmic). One instance when increased catabolic capacity is warranted is when supplies of essential nutrient(s) are exhausted and the cells make the transition to stationary phase and assume a protective mode against various stresses. One of the attributes of stationary phase is a switchover to maintenance metabolism. Among the many genes induced by the σ^s subunit (one of the global regulators in the stationary-phase response [16]) are some enzymes, including those which make osmoprotectants, scavengers and DNA repair enzymes, but also some that break down glycogen, increase gluconeogenesis, and convert pyruvate to acetate ([16] and references cited therein). This last transformation is carried out by pyruvate oxidase (POX) and releases electrons into the respiratory chain.

The demonstration here that EcoVanX is induced by an RpoS-dependent promoter raises the possibility that this is a maintenance metabolic response and focuses on the two D-Ala products as shown in Figure 8a, as energy sources. Akin to the POX reaction, the membranous D-ADH releases two electrons into the respiratory chain for each D-Ala it oxidizes to pyruvate. The tandem action of D-ADH and POX converts each D-Ala to acetate, NH_3, CO_2 and four electrons that generate four equivalents of ATP to power a starving cell.

This hypothesis raises the broader issue of whether periplasmic D-Ala–D-Ala is indeed released from the peptidoglycan and can be recycled back into the cytoplasm, especially in stationary phase. The operon organization and the demonstration of coexpression of *ecovanX* and dipeptide permease genes increases this likelihood. The results presented here, that coexpression of these genes allows growth on exogenous D-Ala–D-Ala is consistent with such retrieval of D-Ala–D-Ala. We note that it remains to be shown that ORFs ABCDE (Figure 4) are indeed D,D-specific, but there has long been evidence that D-Ala–D-Ala and a few selected analogs can be taken up by *E. coli* [35].

In a broad context, Figure 8a shows both D-Ala and also D-Ala–D-Ala as points of metabolic intersection of anabolic and catabolic routes in *E. coli*. In recent years much attention has been duly given to the discovery that about 50% of the periplasmic peptidoglycan (about 3.5 million molecules/cell) is turned over in each *E. coli* generation, GlcNAc-anhydroMurNAc tripeptide and free L-Ala–D-Glu–L-A_2pm tripeptide are the cell-wall fragments that are transported back into the cytoplasm by transmembrane AmpG and MppA and hydrolyzed by the amidase AmpD. The L-Ala–D-Glu–L-A_2pm tripeptide is then recycled [36]. No attention has been given to the fate of the D-Ala released from peptidoglycan tetrapeptide termini or the D-Ala–D-Ala from the uncross-linked peptidogycan pentapeptide termini. Although it has been

Figure 8

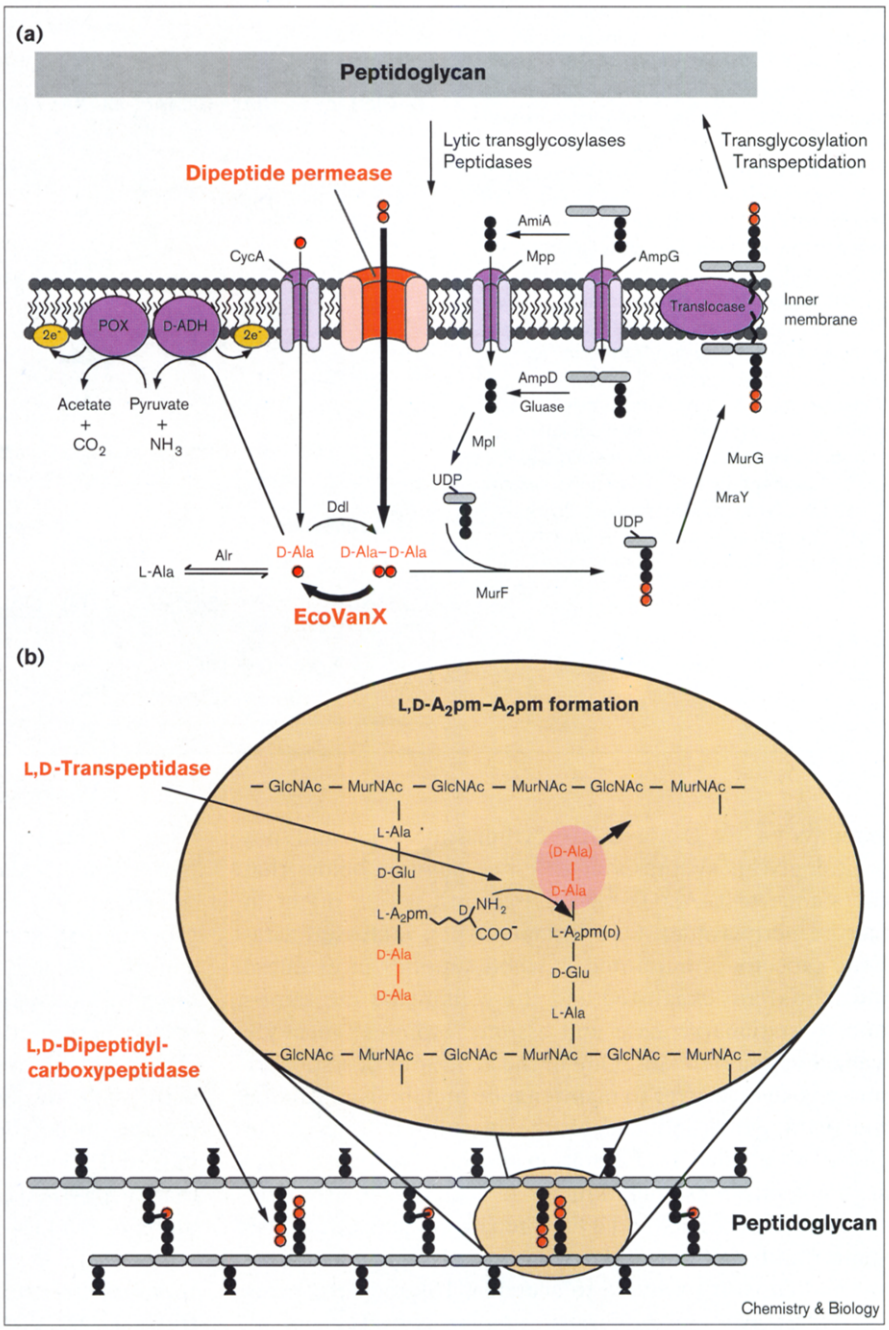

D-Ala and D-Ala–D-Ala as branch point metabolites in *E. coli*. Proposed action of EcoVanX and the putative dipeptide permease. **(a)** Recycling of peptidoglycan turnover products. Peptidoglycan is degraded by several hydrolases (see Figure 7). The periplasmic GlcNAc–MurNAc-tripeptide product can be transported directly into the cytoplasm by AmpG and then converted by AmpD/Glucosaminidase(Gluase) into tripeptide (L-Ala–D-Glu–L-A_2pm: black circles) and disaccharide (GlcNAc–MurNAc, gray ovals) or degraded by AmiA to the disaccharide and tripeptide units (see [37] for review). Periplasmic tripeptide is transported by a specific murein peptide permease (Mpp) [60] or by the oligopeptide permease (Opp) [37]. Tripeptide can be reused directly for the synthesis of peptidoglycan precursors for subsequent cell-wall biosynthesis. The fate of the periplasmic disaccharide is not known. D-Ala (red circle) monomer released from the transpeptidation reaction (D-Ala-D-A_2pm) and the DD-(LD-) carboxypeptidase reaction is transported by the CycA system [61] into the cytoplasm. During stationary phase, periplasmic D-Ala–D-Ala dipeptide might be transported by a novel dipeptide transport system into the cytoplasm where it could be processed by two different pathways: recyclization by MurF for cell-wall biosynthesis or degradation to its monomer by EcoVanX. As a possible route for production of energy during starvation, the D-Ala would be converted to acetate by the sequential action of D-amino acid dehydrogenase (D-ADH) and pyruvate oxidase (POX). D-Ala could also be converted back into D-Ala–D-Ala by the Ddl ligase or into L-Ala necessary for protein synthesis by a racemase (Alr) or into pyruvate/ammonia to be used as a carbon/nitrogen source. **(b)** Possible source of periplasmic D-Ala–D-Ala. During stationary phase, A_2pm–A_2pm cross-linkages increase up to 10% of total cross-linkages [31]. It is predicted that this reaction would release a single monomer of D-Ala [37] or a D-Ala–D-Ala dipeptide moiety. It has been shown that D-Ala–D-Ala is released by an L,D-dipeptidylcarboxypeptidase from peptidogycan precursors [38]. The latter enzyme could also be the A_2pm–A_2pm transpeptidase, the gene and gene product of which have yet to be identified. A_2pm, diaminopimelic acid; GlcNAc, *N*-acetylglucosamine; MurNAc, *N*-acetylmuramic acid.

assumed the A_2pm–A_2pm cross-links that form in stationary phase arise from tetrapeptide chains that release D-Ala [36], in fact the enzyme has not been characterized and it is possible that the substrates are pentapeptide chains, releasing D-Ala–D-Ala in the A_2pm–A_2pm cross-links form (Figure 8b). Such cross-links would then liberate a potential energy source for the starving cell in stationary phase provided that the cells also turn on the genes for retrieval and hydrolysis of the D,D-dipeptide; analogous to burning the walls of the house to generate heat. The L,D-dipeptidylcarboxypeptidase cleaving the L-A_2pm–D-Ala–D-Ala termini at the L-Dap–D-Ala peptide bond, previously described in *E. coli* [37], could in fact be the A_2pm–A_2pm transpeptidase (Figure 8b),

perhaps also turned on in an RpoS-dependent manner. For each D-Ala–D-Ala thus retrieved from the peptidoglycan termini, eight ATPs could be produced by the tandem action of POX and D-ADH suggested in Figure 8a. This might be the reason for switching from L-A_2pm–D-Ala to A_2pm–A_2pm cross-links in stationary phase.

Less is known about the putative physiological function of SynVanX. It clearly exhibits zinc-mediated dipeptidase activity but is also atypical as it can hydrolyze both L-Ala–D-Ala and D-Ala–D-Ala with similar efficiency. No dipeptide permease genes are clustered close to the *synvanX* gene. Given the insensitivity of *Synechocystis* to glycopeptide antibiotics by reason of antibiotic exclusion, it is unlikely that SynVanX plays any immunity-conferring function and more likely that it plays a scavenging role for L,D-and D,D-dipeptide products of cell-wall degradation pathways. As additional bacterial genomes are sequenced, more VanX proteins homologs are likely to be discovered. Indeed, in the gram-positive pathogen *Mycobacterium tuberculosis* there is a VanX homolog, this time with an apparent signal sequence and membrane lipoprotein attachment site (ORF-MTV043.31, accession 2916897, [38]) suggesting that MtuVanX might reside in the membrane.

Significance

The metallodipeptidase VanX (EntVanX) plays an essential role in life-threatening, pathogenic vancomycin-resistant enterococci (VRE) by hydrolyzing the D-Ala–D-Ala dipeptide but not the D-Ala–D-lactate depsipeptide during rerouting of cell-wall intermediates. There is interest in the likely origin of the transposon-encoded *vanX* in VRE and its distribution in other bacteria, both gram-positive and gram-negative. We report on the detection, overproduction and kinetic characterization of three bacterial VanX homologs from the glycopeptide-antibiotic producer *Streptomyces toyocaensis* (StoVanX), from *Escherichia coli* (EcoVanX) and from the cyanobacterium *Synechocystis* sp. strain PCC6803 (SynVanX).

The StoVanX homolog (64% similarity with EntVanX), whose gene is found clustered within a *vanHAX* operon, exhibits similar kinetic parameters to EntVanX, consistent with an antibiotic immunity function in the *S. toyocaensis* producer and indicative of a possible common evolutionary origin. EcoVanX and SynVanX show much lower sequence homology to EntVanX (27% and 16% respectively), are found in gram-negative bacteria that have no comparable susceptibility to vancomycin or need for defense against this antibiotic and show 200-fold elevation in K_M values for D-Ala-D-Ala hydrolysis compared to EntVanX, which suggests a probable role for these enzymes in cell-wall turnover.

Directly downstream of the *ecovanX* gene is a putative dipeptide permease gene cluster, the products of which show capacity to import D-Ala-D-Ala into the cell. These genes form an operon under the control of the stationary phase transcription factor RpoS. The consecutive action of EcoVanX and the membranous D-amino acid dehydrogenase and pyruvate oxidase would allow the cell to utilize D-Ala–D-Ala as an energy source for cell survival under starvation conditions. Periplasmic D-Ala–D-Ala could be provided by the diaminopimelic acid (A_2pm)–A_2pm cross-link action, which substantially increases during stationary phase. This potential energy source could be the reason for switching from L-A_2pm–D-Ala to A_2pm–A_2pm cross-links.

Materials and methods

Materials

Bacteriological media were obtained from Difco Laboratories. Competent *E. coli* strain BL21 (DE3) was purchased from Novagen. Competent *E. coli* strain DH5α and DNase I were purchased from GibcoBRL. Restriction endonucleases, T4 DNA ligase, calf intestinal alkaline phosphatase, and amylose resin were obtained from New England Biolabs. *Pfu* DNA polymerase was purchased from Stratagene. Isopropyl-1-thio-β-D-galactopyranoside (IPTG), L-Ala–D-Ala, D-Ala–L-Ala, L-Ala–D-Gln, L-Ala–β-D-Glu–D-Lys–D-Ala–D-Ala and D-Ala-D-Ala-OMe were purchased from Bachem Biosciences. Kanamycin, ampicillin, chloramphenicol, D-Ala–D-Ala, L-Ala–L-Ala, *N*-acetyl-D-Ala–D-Ala, D-Ala–D-Ala–D-Ala and L-Ala–L-Ala–L-Ala were purchased from Sigma. D-Ala–D-lactate has been synthesized previously in this laboratory [12]. Chelex-100 resin and low molecular weight markers for polyacrylamide gel electrophoresis (PAGE) were obtained from Bio-Rad. Genomic DNA from *Synechocystis* sp. strain PCC6803 was the kind gift of Dr. Louis Sherman (Purdue University). *E. coli* strains and plasmids used in this work are presented in Table 3.

Recombinant DNA methods

Recombinant DNA techniques were performed as described elsewhere [39]. Preparation of plasmid DNA, gel-purification of DNA fragments, purification of PCR-amplified DNA fragments [40,41], and preparation of total RNA were performed using QIAprep® spin plasmid miniprep, QIAEX® II gel extraction, QIAquick™ PCR, and RNeasy® purification kits, respectively (QIAGEN). PCR reactions were carried out as described previously [42] using *Pfu* DNA polymerase. Variations in the general PCR conditions are noted in the text. Splicing by overlap extension (SOE) reactions [43] were carried out similarly using approximately an equimolar ratio (total amount ~50 ng) of each gel-purified PCR-amplified DNA fragments to be joined as template. The fidelity of the SOE- or PCR-amplified DNA fragments was verified by nucleotide sequencing of the respective cloned fragments. Oligonucleotide primers were obtained from Integrated DNA Technologies, and DNA sequencing was performed on double-stranded DNA by the Molecular Biology Core Facility of the Dana Farber Cancer Institute (Boston, MA).

Construction of expression vectors for MBP–VanX fusion proteins

The expression vector for MBP–VanX (MBP–EntVanX$_A$) fusion protein (pIADL14 [9]) was used to construct vectors for the expression of the genes encoding StoVanX, EcoVanX and SynVanX. The *stovanX* [11] and *synvanX* (ORF-slr1679, accession 1653448 [44]) genes were PCR-amplified from pBlutoyVnX5.4 and *Synechocystis* genomic DNA using the primer pairs 2033/1034, and 2045/1037, respectively (Table 4). For amplification of the *ecovanX* gene (ORF-f193, accession 1787763 [45]), a single colony of *E. coli* strain BW24320 (Table 3) was resuspended in 40 µl of 10 mM Tris (pH 8.3), 50 mM KCl, 2.5 mM $MgCl_2$, 20 mM DTT and 1.8 µM SDS and incubated for 30 min at 37°C. Supernatant from the lysed cells (5 µl) was used as the template for PCR using the primer pair 2032/1033 (Table 4). PCR products were digested with *Nde*I and

Table 3

***Escherichia coli* strains and plasmids used in this work.**

Construction	Description	Reference/Source
Strains*		
BL21 (DE3)	F–, *ompT*, $hsdS_B$, (r_{B-},m_{B-}), *gal*, *dcm*, λ(DE3)	Novagen
BW21480	*lacI*^{q} $rrnB_{T14}$ Δ$lacZ_{WJ16}$ *rpoS*(Am)	[54]
BW22653	*lacI*^{q} $rrnB_{T14}$ Δ$lacZ_{WJ16}$	†
BW24320	*lacI*^{q} $rrnB_{T14}$ Δ$lacZ_{WJ16}$ Δ*phoBR580* Δ*creABCD154* Δ$araBAD_{AH37}$ Δ$rhaBAD_{LD78}$	‡
BW25113	*lacI*^{q} $rrnB_{T14}$ Δ$lacZ_{WJ16}$ *hsd*R514 Δ$araBAD_{AH33}$ Δ$rhaBAD_{LD78}$	‡
BW25141	*lacI*^{q} $rrnB_{T14}$ Δ$lacZ_{WJ16}$ Δ*phoBR580 hsdR514* Δ$araBAD_{AH33}$ Δ$rhaBAD_{LD78}$ *uidA* (Δ*MluI*)::pir$^+$ *rpoS*(Am) $endA_{BT333}$ *galU95 recA1*	‡
DH5α	F–, ϕ80d*lacZ*Δ*M15*, Δ(*lacZYA–argF*)*U169*, *deoR*, *recA1*, *endA1*, *hsdR17*(r_K^-, m_K^+), *phoA*, *supE44*, λ$^-$, *thi-1*, *gyrA96*, *relA1*	Stratagene
IADL307	Like BW25113 except *attλ*::pIADL93 (P_{lac}–*ecovanX*)	This study
IADL310	Like BW22653 except *attλ*::pIADL96 ($P_{ecovanX}$–*lacZ*)	This study
IADL313	Like BW21480 except *attλ*::pIADL96 ($P_{ecovanX}$–*lacZ*)	This study
IADL318	Like BW25113 except *attλ*::pIADL101 (P_{lac}–*entvanX*$_A$)	This study
IADL319	Like BW25113 except *attHK022*::pIADL100 (P_{lac}–*dipeptide permease*)	This study
IADL321	Like IADL307 except *attHK022*::pIADL100 (P_{lac}–*dipeptide permease*)	This study
NM522	*supE thi-1* Δ(*lac-proAB*) Δ(*mcrB-hsdSM*)5 (r_K^-, m_K^-) [F′ *proAB lacI*^{q}*ZΔM15*]	Stratagene
SM10λ *pir*	*thi thr leu tonA lacY supE recA*::RP4-2Tc::Mu *kan λpir*	[55]
SPNM-1	Like NM522 except rifampicin	This study
SP14-2	Like SPNM-1 except *ecovanX::cat*	This study
XL1-Blue	*recA1 endA1 gyrA96 thi-1 hsdR17 supE44 relA1 lac* [F′ *proAB lacI*^{q}*ZΔM15*] Tn*10* (Tet^r)]	Stratagene
Plasmids§		
pACYC184	ori_{p15A}, *cat*, *tet*	NEB#
pAH125	*lacZ* transcriptional fusion vector, $attP_\lambda$, $oriR_{R6K\gamma}$, *kan*	¶
pBlutoyVnX5.4	5′-end *ddlM*, *stovanX* genes in pBluescript, ori_{MB1}, *bla*	[11]
pDEB2	P_{lac}–RpoS producing plasmid, ori_{MB1}, *bla*	[56]
pIADL14	P_{T7}–MBP–EntVanXA overproducing plasmid, ori_{MB1}, *kan*	[9]
pIADL55	P_{T7}–MBP–EcoVanX overproducing plasmid, ori_{MB1}, *kan*	This study
pIADL58	P_{T7}–MBP–SynVanX overproducing plasmid, ori_{MB1}, *kan*	This study
pIADL60	P_{T7}–MBP–StoVanX overproducing plasmid, ori_{MB1}, *kan*	This study
pIADL70	*ecovanX* gene, $attP_\lambda$, $oriR_{R6K\gamma}$, *kan*	¥
pIADL72	*orfABCD* and 5′-end *orfF* dipeptide permease genes in pUC19	This study
pIADL73	3′-end *orfF* dipeptide permease gene in pUC19	This study
pIADL74	*orfABCDF* dipeptide permease genes in pUC19	This study
pIADL75	P_{rhaB}–geneIV, $attP_{HK022}$, $oriR_{R6K\gamma}$, *cat*	¥
pIADL76	P_{rhaB}–dipeptide permease, $attP_{HK022}$, $oriR_{R6K\gamma}$, *cat*	This study
pIADL93	P_{lac}–EcoVanX producing plasmid, $attP_\lambda$, $oriR_{R6K\gamma}$, *kan*	This study
pIADL96	$P_{ecovanX}$–LacZ fusion, $attP_\lambda$, $oriR_{R6K\gamma}$, *kan*	This study
pIADL100	P_{lac}–dipeptide permease, $attP_{HK022}$, $oriR_{R6K\gamma}$, *cat*	This study
pIADL101	P_{lac}–EntVanX$_A$, $attP_\lambda$, $oriR_{R6K\gamma}$, *kan*	This study
pINT-ts	P_R-λ integrase producing plasmid, $ori_{pSC101\text{-}ts}$, *bla*	[57]
pKNG101	*sacBR*, mob_{RK2}, $oriR_{R6K\gamma}$, str_{AB}	[58]
pKXC-5	1.5 *kb–ecovanX::cat-1.2 kb*, *sacBR*, mob_{RK2}, $oriR_{R6K\gamma}$, str_{AB}	This study
pSPORT1	P_{lac}, ori_{MB1}, *bla*	Gibco BRL
pUC18/19	ori_{MB1}, bla	NEB
pUEX	*1.5 kb–ecovanX–1.2 kb*, ori_{MB1}, *bla*	This study
pUEXC	*1.5 kb–ecovanX::cat-1.2 kb*, ori_{MB1}, *bla*	This study

*All *E. coli* strains listed are derived from strain K-12, except for BL21(DE3) which is derived from strain B. †Jiang, W., Haldimann, A. & Wanner, B.L., unpublished strain. ‡Haldimann, A. & Wanner, B.L., unpublished strains and vector. §Plasmid with $oriR_{R6K\gamma}$ required *E. coli* strain harboring the *pir* gene for replication; *orf*ABCDF, see Figure 4. #New England BioLabs. ¶S.K. Kim, A. Haldimann and B.L. Wanner, unpublished vectors. ¥I.A.D.L. & C.T.W., unpublished vectors.

*Hin*dIII, and the resulting *vanX* homolog-containing DNA fragments were gel-purified and cloned into pIADL14. The resulting plasmids pIADL55, pIADL58 and pIADL60 encode MBP fusions with EcoVanX, SynVanX and StoVanX, respectively. *E. coli* strains DH5α and BL21(DE3) were used as cloning and expression hosts.

Overproduction and purification of MBP–VanX homologs

Overproduction and purification of the MPB–VanX homologs were performed as described previously [9] with the following two modifications: buffer A contained 300 mM NaCl, and $ZnSO_4$ (10 mM stock solution) was added to the purified protein to a final concentration of 200 μM

Table 4

Oligonucleotide primers for PCR.

Comment	Code	5′–3′ Nucleotide sequence
P_{T7}–StoVanX	2045	***CG****CAAGCTT*CTACATGATGGGGAAATCGAAGT
P_{T7}–StoVanX	1037	***AGGATCCCAT***ATGAAGCCGACGGAGTCCATGA
P_{T7}–EcoVanX	2032	CAGGAACCG***CA***TATGTCGGATACCACCGAACTGG
P_{T7}–EcoVanX	1033	CAGTTTC***AAGC***TTAACTGACGTGCTGTGTGCC
P_{T7}–SynVanX	2033	***CAGGAACCGCAT***ATGTCCTTTGATACCCCGCTCAAAC
P_{T7}–SynVanX	1034	***CAGTTTCAAGCTT***CATTCAACCCGGCCGTAGTAGG
$P_{ecovanX}$	2081	***GGCCTGCA***GATGAGCAGCGTGTTACCGCTG
$P_{ecovanX}$	1039	CGG***AATTC***GTATAAGACAAAAATTGCTGCGCTTCC
Dipeptide permease, 5′-end	2060	CAGGAA***TTCCAT***ATGAAGAGATCGATATCGTTTC
Dipeptide permease, 5′-end	1049	CCGTC***TAG***AGCAGACGCATAATCAG
Dipeptide permease, 3′-end	2063	CACG***AAT***TCAACAATGTGTCCTTGC
Dipeptide permease, 3′-end	1052	CGTT***CTAGACGCG***TCTACAGCGCCCGCCAGC
Dipeptide permease, *Nde*I–	1051	GATCGCTCAT***G***TGACGTATCACCGAG
Dipeptide permease, *Nde*I–	2065	CTCGGTGATACGTCA***C***ATGAGCGAT
P_{lac}–EcoVanX	2044	AGT***TCTAGAGGATC***CTTAACTGACGTGCTGTGTG
P_{lac}–EcoVanX	1053	GGACTTTCTGCGCGTCTGATTAAGC
P_{lac}	1071	***CTCCTCTACATAT GTATATCT***CCTGTGTGAAATTGTTATCCGCTCAC
P_{lac}	2077	G***GGC***AT***G***CATTAATGCAGCTGGCACGACAGG
attλ	1023	GGCATCACGGCAATATAC
attλ	2023	TCTGGTCTGGTAGCAATG
attHK022	1024	GGAATCAATGCCTGAGTG
attHK022	2024	GGCATCAACAGCACATTC
att-plasmid	1027	ACGAGTATCGAGATGGCA
att-plasmid	2027	ACTTAACGGCTGACATGG
$up_{ecovanX}$	4001	***GTCACGGTCGAC***ACCGGTCTGCCAAATCGCAA
$down_{ecovanX}$	3001	***GTCA***CG***G***GA***TC***CCAGTTGCCAATCGCAATGTCGTA
cat	4002	***GGTCACGCTCAGCTATAA***GAGTTATCGAGATTTTCAGGAGCTA
cat	3002	***TA***ACG***A***TGC***TGAGC***AGGGCACCAATAACTGCCTT
$RT\text{–}PCR_{ecovanX\text{-}orfA}$	4003	GTCGGATACCACCGAACTGGTTGATTT
$RT\text{–}PCR_{ecovanX\text{-}orfA}$	3003	GCGCTTTGCTGTTATTCAGATACAGATAGGTAA
$RT\text{–}PCR_{orfB\text{-}orfF}$	4004	TTGCCGTCGTGGTTTCATTTGCTTA
$RT\text{–}PCR_{orfB\text{-}orfF}$	3004	AAGCGAAGAGAGCGGGTCCTGAA

Mismatches are bold and italicized.

and incubated for 1 hour on ice prior to dialysis. The yield of pure MBP-VanX homolog proteins obtained from a 1 l culture of induced *E. coli* BL21(DE3) cells was ~40 mg.

Protein quantitation and SDS–PAGE

Concentrations of pure protein were determined by using UV–Vis spectroscopy (ε_{280} = 118,720 $M^{-1}cm^{-1}$ [MBP–EntVanX], ε_{280} = 115,740 $M^{-1}cm^{-1}$ [MBP-StoVanX], ε_{80} = 93,280 $M^{-1}cm^{-1}$ (MBP–EcoVanX) and ε_{280} = 118,720 $M^{-1}cm^{-1}$ [MBP–SynVanX]). The extinction coefficients were calculated using a modification of the Edelhoch method [46,47]. Proteins were separated by SDS–PAGE using a discontinuous Tris/glycine buffer [48] with 10% acrylamide resolving gels and 5% acrylamide stacking gels containing 0.1% SDS.

Assays for enzyme activity and ICP-metal analysis

Peptidase activity was measured in 50 mM Tris (pH 8.0) at 37°C according to published procedures [12] using the modified cadmium-ninhydrin assay method, which detects the concentration of free D-Ala [49]. Protein samples were prepared for metal analysis as described earlier [9] except that dialysis was performed with three changes of buffer. Protein samples were analyzed for metal content at the University of Georgia Chemical Analysis Laboratory (Athens, GA). The detection limit for zinc was determined to be <1 ppb.

Construction of E. coli *strains harboring promoter fusion (ecovanX) with lacZ*

A 282 bp DNA segment upstream of the Shine–Delgarno (SD) sequence of the *ecovanX* gene (Figure 4) was fused with the *lacZ* gene. This DNA fragment included a putative transcriptional terminator and the last 9 coding amino acids of a hypothetical gene (ORF-f807, accession 1787765 [45]). The 282 bp DNA fragment was PCR-amplified from a single colony of *E. coli* strain BW24320 (Table 4) as described above using the primer pair 2081/1039 (Table 4) with an annealing temperature (T_{an}) of 60°C. The PCR product was digested with *Eco*RI and *Pst*I, gel-purified and cloned into pAH125, to create pIADL96. The *E. coli* strain BW25141 (Table 3) contains a chromosomal copy of the *pir* gene (π protein) required for replication (acting in trans) of this $oriR_{R6K\gamma}$-based plasmid [50] and was used as the cloning host. The pIADL96 plasmid was integrated into *attλ* in *E. coli* strains BW21480 and BW22653 (Table 3) as described earlier [50]. Single integrations were verified by PCR using the primers 1023/2023/1027/2027 with a T_{an} of 60°C. The resulting *E. coli* strains, IADL310 and IADL313, contain a single chromosomal copy of the promoter fusion construct at the *attλ* site (Table 3).

Assay of the promoter fusion with lacZ

A single colony of *E. coli* strain IADL310 or IADL313 was used to inoculate 5 ml of LB media containing 5 μg/ml of kanamycin and grown

overnight at 37°C. The cultures were diluted 10-fold in LB media and growth was continued for 30 min at 37°C. This step was repeated twice after which the cultures were diluted 10-fold into 50 ml of LB media and growth was followed at 37°C. Samples were taken at different times over 24 h for determination of the β-galactosidase activity and for cell density measurements at 600 nm. β-galactosidase activity was assayed with *ortho*-nitrophenyl-galactopyranoside in quantitative liquid culture assays as described by Miller [51]. The assay was performed in triplicate from separate colonies.

Analysis of the transcript for ecovanX *and the dipeptide permease cluster genes*

E. coli strain NM522 was grown in 3 ml LB at 37°C to an OD_{600} of 0.78 (exponential phase) and 2.32 (stationary phase) and used for preparation of total RNA. The preparations of RNA were further treated by DNase I and amplified by RT–PCR using the Takara BcaBest RNA PCR kit (Takara Shuzo Co.) as described by the manufacturer and primer pairs 4003/3003 and 4004/3004 (T_{an} of 62°C). Identity of the PCR products was confirmed by restriction mapping.

Construction of E. coli *strains expressing* ecovanX, entvanX_A *and a putative dipeptide permease system cluster genes*

The *ecovanX* gene was PCR-amplified from pIADL55 using the primer pair 1053/2044 (Table 4). The PCR product was digested with *Nde*I and *Bam*HI, gel-purified and cloned into pAH135, to create pIADL70. P_{lac} was PCR-amplified from pSPORT1 using the primer pair 1071/2077 (Table 4). The PCR product was digested with *Nde*I and *Sph*I, gel-purified and cloned into pIADL70, to create pIADL93. The *entvanX*$_A$ gene was cloned into pIADL93 at the *Nde*I and *Xma*I sites from pIADL14 to create pIADL101. Plasmids pIADL93 and pIADL101 were then integrated into *attλ* of *E. coli* strain BW25113 (Table 3) as described earlier [50] to create strains IADL307 and IADL318, respectively. Single integration was verified by PCR using the primers 1023/2023/2027/1027 (T_{an} of 60°C). *E. coli* strain BW25141 was used as the cloning host.

The entire putative dipeptide permease cluster of genes found just 13 bp downstream of the *ecovanX* gene (Figure 4) was cloned from *E. coli* strain BW24320 by colony PCR (see above). The 5′-end sequence was PCR-amplified from a single colony using the primer pair 2060/1049 (Table 4) with a 10 min extension time (t_{ex}) and a T_{an} of 48°C, producing a 3660 bp DNA fragment. The PCR product was digested with *Nde*I and *Xba*I, gel-purified and cloned into pUC19, to create pIADL72. At the 3′-end sequence, an internal *Nde*I restriction site was removed by silent mutagenesis using the SOE method. For the first round of PCR, the sequence upstream and downstream of the *Nde*I restriction site were separately amplified using the primer pairs 2063/1051 and 2065/1052 (Table 4), respectively (t_{ex} of 8 min, T_{an} of 48°C). The resulting DNA fragments (1547 bp and 333 bp, respectively) were gel-purified and subjected to a second round of PCR using the primer pair 2063/1052 with the above conditions. The SOE-purified DNA fragment (1854 bp) was digested with *Eco*RI and *Xba*I and cloned into pUC19, to create pIADL73. The 5′-end sequence of the cluster was then subcloned into pIADL73 at the *Sac*II and *Nde*I sites to create pIADL74. The entire dipeptide permease genes cluster was subcloned into pIADL75 at the *Nde*I and *Mlu*I sites, to create pIADL76. Plasmid pIADL75 (I.A.D.L. and C.T.W. unpublished vector) is a pSK49 based plasmid [50] possessing the P_{rhaB}, the *cat* gene, the *attP*$_{HK022}$ site for integration into the chromosome into *attHK022* and *ori*$R_{R6K\gamma}$ (A. Haldimann and B.L. Wanner, unpublished observations). P_{lac} was subcloned from pIADL93 into pIADL76 at the *Nde*I/*Sph*I sites to create pIADL100. Plasmid pIADL100 was integrated into *attHK022* of *E. coli* strains BW25113 and IADL307 as described earlier [50] to create strains IADL319 and IADL321, respectively. Single integration was confirmed by PCR using the primers 1024/2024/1027/2027 (T_{an} of 60°C).

Insertional inactivation of the chromosomal ecovanX *gene*

Inactivation of *ecovanX* gene was accomplished by insertion of the *cat* gene into the *Bpu*1102I site of *ecovanX*. The chromosomal region harboring the *ecovanX* gene, plus 1.5 kb upstream and 1.2 kb downstream sequences, was PCR-amplified from *E. coli* strain XL1 Blue, using the primer pair 4001/3001 (Table 4). The PCR product was cloned into pUC18 at the *Sal*I and *Bam*HI sites to create pUEX. The *cat* gene was PCR-amplified from pACYC184 using the primer pair 4002/3002 (Table 4) and cloned at the *Bpu*1102I site of *ecovanX* in pUEX to create pUEXC. The *Sal*I-*Bam*HI region of pUEXC was then subcloned into the suicide vector pKNG101 to create pKXC-5 using *E. coli* strain SM10 λ *pir* (permissive host strain for pKNG101) as the host (donor strain). *E. coli* strain NM522 was selected for resistance to 100 μg/ml rifampicin to produce SPNM-1 (acceptor strain). Recombination was performed using conjugation by the following procedure: SM10 λ *pir*/pKXC-5 (LB, 40 μg/ml chloramphenicol, 50 μg/ml streptomycin) and SPNM-1 (LB, 100 μg/ml rifampicin) cells were separately grown overnight at 37°C. The overnight cultures were then diluted 1:10 in 1 ml LB to give a final OD_{600} of c.a. 0.5, centrifuged, and resuspended in 600 μl antibiotic-free LB. A 200 μl sample from each culture was mixed, centrifuged, the pellets resuspended in 10 μl LB and spotted onto a prewarmed LB plate which was then incubated at 37°C for 5 h to allow conjugation (individual cultures were used as controls). Spotted bacteria were scraped and resuspended in 600 μl LB, plated on LB plates (100 μg/ml rifampicin, 25 μg/ml chloramphenicol, and 10 μg/ml streptomycin) and incubated at 37°C overnight. Colonies were grown in 3 ml LB (same antibiotics as the plates) at 37°C for 6 h and streaked on LB agar containing 25 μg/ml chloramphenicol and 5% sucrose to force a second crossover, removing the nonhomologous portion of the integrated pKXC-5 plasmid from the chromosome. Colonies from this experiment were replica plated with and without streptomycin to confirm loss of plasmid DNA. Recombinants were analyzed by Southern blot and PCR to confirm insertion of *cat*.

Homology modeling of EcoVanX using EntVanX$_A$ *as the template*

Homology modeling was performed using the crystal structure of EntVanX$_A$ [10], a sequence alignment of the EntVanX$_A$ and EcoVanX sequences generated using Clustal W [52], and the Modeller program [53].

Acknowledgements

We thank Karl A. Reich (Abbott) for help in the construction of the *ecovanX* knockout strain. We thank Roberto Kolter and Manuel Espinosa-Urgel (Harvard Medical School), Francis C. Neuhaus (Northwestern University), Ping Zhong (Abbott), and Ranabir Sinha Roy and other members of the Walsh laboratory for helpful discussions. We also thank Gerry D. Wright and C. Gary Marshall (McMaster University) for communicating information about *S. toyocaensis* VanX. I.A.D.L. wishes to acknowledge the Natural Sciences and Engineering Research Council of Canada for Postdoctoral Fellowship support. This research was supported in part by a financial grant from Abbott Laboratories to C.T.W.

References

1. Neu, H.C. (1992). The crisis in antibiotic resistance. *Science* **257**, 1064-1073.
2. Tomasz, A. (1994). Multiple-antibiotic-resistant pathogenic bacteria. A report on the Rockefeller University Workshop. *N. Engl. J. Med.* **330**, 1247-1251.
3. Swartz, M.N. (1994). Hospital-acquired infections: diseases with increasingly limited therapies. *Proc. Natl Acad. Sci.* **91**, 2420-2427.
4. Gaynes, R.P., Edwards, J.R., Jarvis, W.R., Culver, D.H., Tolson, J.S. & Martone, W.J. (1996). Nosocomial infections among neonates in high-risk nurseries in the United States. National Nosocomial Infections Surveillance System. *Pedriatrics* **98**, 357-361.
5. Arthur, M. & Courvalin, P. (1993). Genetics and mechanisms of glycopeptide resistance in enterococci. *Antimicrob. Agents Chemother.* **37**, 1563-1571.
6. Arthur, M., Molinas, C., Depardieu, F. & Courvalin, P. (1993). Characterization of Tn1546, a Tn3-related transposon conferring glycopeptide resistance by synthesis of depsipeptide peptidoglycan precursors in *Enterococcus faecium* BM4147. *J. Bacteriol.* **175**, 117-127.
7. Reynolds, P.E., Depardieu, F., Dutka-Malen, S., Arthur, M. & Courvalin, P. (1994). Glycopeptide resistance mediated by enterococcal transposon Tn1546 requires production of VanX for hydrolysis of D-alanyl–D-alanine. *Mol. Microbiol.* **13**, 1065-1070.

8. Walsh, C.T., Fisher, S.L., Park, I.-S., Prahalad, M. & Wu, Z. (1996). Bacterial resistance to vancomycin: five genes and one missing hydrogen bond tell the story. *Chem. Biol.* **3**, 21-28.
9. McCafferty, D.G., Lessard, I.A.D. & Walsh, C.T. (1997). Mutational analysis of potential zinc-binding residues in the active site of the enterococcal D-Ala-D-Ala dipeptidase VanX. *Biochemistry* **36**, 10498-10505.
10. Bussiere, D.E., Pratt, S.D., Katz, L., Severin, J.M., Holzman, T. & Park, C. (1998). The structure of VanX reveals a novel amino-dipeptidase involved in mediating transposon-based vancomycin resistance. *Mol. Cell* **2**, 75-84.
11. Marshall, G.C., Lessard, I.A.D., Park, I.-S. & Wright, G.D. (1998). Glycopeptide antibiotic resistance genes in glycopeptide-producing organisms. *Antimicrob. Agents Chemother.*, in press.
12. Wu, Z., Wright, G.D. & Walsh, C.T. (1995). Overexpression, purification, and characterization of VanX, a D-,D-dipeptidase which is essential for vancomycin resistance in *Enterococcus faecium* BM4147. *Biochemistry* **34**, 2455-2463.
13. Burley, S.K. & Petsko, G.A. (1985). Aromatic-aromatic interaction: a mechanism of protein structure stabilization. *Science* **229**, 23-28.
14. Olson, E.R., Dunyak, D.S., Jurss, L.M. & Poorman, R.A. (1991). Identification and characterization of *dppA*, an *Escherichia coli* gene encoding a periplasmic dipeptide transport protein. *J. Bacteriol.* **173**, 234-244.
15. Espinosa-Urgel, M., Chamizo, C. & Tormo, A. (1996). A consensus structure for sigma S-dependent promoters. *Mol. Microbiol.* **21**, 657-659.
16. Hengge-Aronis, R. (1996). Regulation of gene expression during entry into stationary phase. In *Escherichia coli and Salmonella, cellular and molecular biology.* (Neidhardt *et al.* eds), pp. 1497-1512, ASM Press, Washington.
17. Hengge-Aronis, R., Klein, W., Lange, R., Rimmele, M. & Boos, W. (1991). Trehalose synthesis genes are controlled by the putative sigma factor encoded by *rpoS* and are involved in stationary-phase thermotolerance in *Escherichia coli*. *J. Bacteriol.* **173**, 7918-7924.
18. Lange, R. & Hengge-Aronis, R. (1991). Growth phase-regulated expression of bolA and morphology of stationary-phase *Escherichia coli* cells are controlled by the novel sigma factor sigma S. *J. Bacteriol.* **173**, 4474-4481.
19. Lambert, M.P. & Neuhaus, F.C. (1972) Factors affecting the level of alanine racemase in *Escherichia coli*. *J. Bacteriol.* **109**, 1156-1161.
20. Olsiewski, P.J., Kaczorowski, G.J. & Walsh C.T. (1980). Purification and properties of D-amino acid dehydrogenase, an inducible membrane-bound iron-sulfur flavoenzyme from *Escherichia coli* B. *J. Biol. Chem.* **255**, 4487-4494.
21. Wright, G.D., Holman, T.R. & Walsh, C.T. (1993). Purification and characterization of VanR and the cytosolic domain of VanS: a two-component regulatory system required for vancomycin resistance in *Enterococcus faecium* BM4147. *Biochemistry* **32**, 5057-5063.
22. Bugg, T.D.H., Dutka-Malen, S., Arthur, M., Courvalin, P. & Walsh, C.T. (1991). Identification of vancomycin resistance protein VanA as a D-alanine:D-alanine ligase of altered substrate specificity. *Biochemistry* **30**, 2017-2021.
23. Bugg, T.D.H., Wright, G.D., Dutka-Malen, S., Arthur, M., Courvalin, P. & Walsh, C.T. (1991). Molecular basis for vancomycin resistance in *Enterococcus faecium* BM4147: biosynthesis of a depsipeptide peptidoglycan precursor by vancomycin resistance proteins VanH and VanA. *Biochemistry* **30**, 10408-10415.
24. Wright, G.D., Molinas, C., Arthur, M., Courvalin, P. & Walsh, C.T. (1992). Characterization of vanY, a DD-carboxypeptidase from vancomycin-resistant *Enterococcus faecium* BM4147. *Antimicrob. Agents Chemother.* **36**, 1514-1518.
25. Arthur, M., Depardieu, F., Snaith, H.A., Reynolds, P.E. & Courvalin, P. (1994). Contribution of VanY D,D-carboxypeptidase to glycopeptide resistance in *Enterococcus faecalis* by hydrolysis of peptidoglycan precursors. *Antimicrob. Agents Chemother.* **38**, 1899-1903.
26. Duez, C., Lakaye, B., Houba, S., Dusart, J. & Ghuysen, J.M. (1990). Cloning, nucleotide sequence and amplified expression of the gene encoding the extracellular metallo (Zn) DD-peptidase of *Streptomyces albus* G. *FEMS Microbiol. Lett.* **59**, 215-219.
27. Marshall, G.C. & Wright, G.D. (1997). The glycopeptide antibiotic producer *Streptomyces toyocaensis* NRRL 15009 has both D-alanyl-D-alanine and D-alanyl-D-lactate ligases. *FEMS Microbiol. Lett.* **157**, 295-299.
28. Höltje, J.-V. & Tuomanen, E.I. (1991). The murein hydrolases of *Escherichia coli*: properties, functions and impact on the course of infections *in vivo*. *J. Gen. Microbiol.* **137**, 441-454.
29. Shockman, G.D. & Höltje, J.-V. (1994). Microbial peptidoglycan (murein) hydrolases. In *Bacterial Cell Wall.* (Ghuysen, J.M. & Hakenbeck, R., eds), pp. 131-163, Elsevier, Amsterdam.
30. Tuomanen, E., Markiewicz, Z. & Tomasz, A. (1988). Autolysis-resistant peptidoglycan of anomalous composition in amino-acid-starved *Escherichia coli*. *J. Bacteriol.* **170**, 1373-1376.
31. Goodell, E.W. & Schwarz, U. (1985). Release of cell wall peptides into culture medium by exponentially growing *Escherichia coli*. *J. Bacteriol.* **162**, 391-397.
32. Goodell, E.W. (1985). Recycling of murein by *Escherichia coli*. *J. Bacteriol.* **163**, 305-310.
33. Vacheron, M.-J., Guinand, M. & Michel, G. (1978). Mise en évidence au cours de la sporulation de *Bacillus sphaericus* d'une activité dipeptidasique sur des substrats constituants du peptidoglycane. *FEMS Microbiol Lett.* **3**, 71-75.
34. Vacheron, M.-J., Guinand, M., Françon, A. & Michel, G. (1979). Charactérisation d'une nouvelle endopeptidase spécifique des liaisons γ-D-glutamyl-L-lysine and γ-D-glutamyl-(L)meso-diaminopimélate de substrats peptidoglycaniques, chez *Bacillus sphaericus* 9602 au cours de la sporulation. *Eur. J. Biochem.* **100**, 189-196.
35. Neuhaus, F.C., Goyer, S. & Neuhaus, D.W. (1977). Growth inhibition of *Escherichia coli* W by D-norvalyl-D-Alanine: an analogue of D-alanine in position 4 of the peptide subunit of peptidoglycan. *Antimicrob. Agents Chemother.* **11**, 638-644.
36. Höltje, J.-V. (1998). Growth of the stress-bearing and shape-maintaining murein sacculus of *Escherichia coli*. *Microbiol. Mol. Biol. Rev.* **62**, 181-203.
37. Gondré, B., Flouret, B. & van Heijenoort, J. (1973). Release of D-alanyl-D-alanine from the precursor of the cell wall peptidoglycan by a peptidase of *Escherichia coli* K 12. *Biochimie* **55**, 685-691.
38. Philipp, W.J., *et al.*, & Cole, S.T. (1996). An integrated map of the genome of the tubercle bacillus, *Mycobacterium tuberculosis* H37Rv, and comparison with *Mycobacterium leprae*. *Proc. Natl Acad. Sci. USA* **93**, 3132-3137.
39. Sambrook, J. Fritsch, E.F. & Maniatis, T. (1989). *Molecular Cloning: A Laboratory Manual*, 2nd Ed., Cold Spring Harbor Laboratory, Cold Spring Harbor, NY.
40. Saiki, R.K., *et al.*, & Erlich, H.A. (1988). Primer-directed enzymatic amplification of DNA with a thermostable DNA polymerase. *Science* **239**, 487-491.
41. Saiki, R.K., *et al.*, & Arnheim, N. (1985). Enzymatic amplification of beta-globin genomic sequences and restriction site analysis for diagnosis of sickle cell anemia. *Science* **230**, 1350-1354.
42. Lessard, I.A.D. & Perham, R.N. (1994). Expression in *Escherichia coli* of genes encoding the E1α and E1β subunits of the pyruvate dehydrogenase complex of *Bacillus stearothermophilus* and assembly of a functional E1 component ($\alpha^2\ \beta^2$) *in vitro*. *J. Biol. Chem.* **269**, 10378-10383.
43. Ho, S.N., Hunt, H.D., Horton, R.M., Pullen, J.K. & Pease, L.R. (1989). Site-directed mutagenesis by overlap extension using the polymerase chain reaction. *Gene* **77**, 51-59.
44. Kaneko, T., *et al.*, & Tabata, S. (1996). Sequence analysis of the genome of the unicellular cyanobacterium *Synechocystis* sp. strain PCC6803. II. Sequence determination of the entire genome and assignment of potential protein-coding regions. *DNA Res.* **3**, 109-136.
45. Blattner, F.R., *et al.*, & Shao, Y. (1997). The complete genome sequence of *Escherichia coli* K-12. *Science* **277**, 1453-1474.
46. Edelhoch, H. (1967). Spectroscopic determination of tryptophan and tyrosine in proteins. *Biochemistry* **6**, 1948-1954.
47. Pace, C.N., Vajdos, F. Fee, L., Grimsley, G. & Gray, T. (1995). How to measure and predict the molar absorption coefficient of a protein. *Protein Sci.* **4**, 2411-2423.
48. Laemmli, U.K. (1970). Cleavage of structural proteins during the assembly of the head of bacteriophage T4. *Nature* **227**, 680-685.
49. Doi, E., Shibata, D. & Matoba, T. (1981). Modified colorimetric ninhydrin methods for peptidase assay. *Anal. Biochem.* **118**, 173-184.
50. Haldimann, A., Prahalad, M.K., Fisher, S.L., Kim, S.K., Walsh, C.T. & Wanner, B.L. (1996). Altered recognition mutants of the response regulator PhoB: a new genetic strategy for studying protein-protein interactions. *Proc. Natl Acad. Sci. USA* **93**, 14361-14366.
51. Miller, J.H. (1972). *Experiments in Molecular Genetics.* Cold Spring Harbor Laboratory, Cold Spring Harbor, N. Y.
52. Thompson, J.D., Higgins, D.G., & Gibson, T.J. (1994). CLUSTAL W: improving the sensitivity of progressive multiple sequence alignment through sequence weighting, position-specific gap penalties and weight matrix choice. *Nucl. Acids. Res.* **22**, 4673-4680.

53. Sali, A. & Blundell, T.L. (1993). Comparative protein modeling by satisfaction of spatial restraints. *J. Mol. Biol.* **234**, 779-815.
54. Haldimann, A., Daniels, L.L., & Wanner, B.L. (1998). Use of new methods for construction of tightly regulated arabinose and rhamnose promoter fusions in studies of the *Escherichia coli* phosphate regulon. *J. Bacteriol.* **180**, 1277-1286.
55. Miller, V.L. & Mekalanos, J.J. (1988) A novel suicide vector and its use in construction of insertion mutations: osmoregulation of outer membrane proteins and virulence determinants in *Vibrio cholerae* requires *toxR*. *J. Bacteriol.* **170**, 2575-2583.
56. Bohannon, D.E., *et al.*, & Kolter, R. (1991). Stationary-phase-inducible "gearbox" promoters: differential effects of *katF* mutations and role of σ^{70}. *J. Bacteriol.* **173**, 4482-4492.
57. Hasan, N., M. Koob & W. Szybalski. (1994). *Escherichia coli* genome targeting, I. Cre-lox-mediated *in vitro* generation of ori- plasmids and their *in vivo* chromosomal integration and retrieval. *Gene* **150**, 51-56.
58. Kaniga, K. Delor, I., Cornelis, G.R. (1991). A wide-host-range suicide vector for improving reverse genetics in gram-negative bacteria: inactivation of the *blaA* gene of Yersinia enterocolitica. *Gene* **109**, 137-141.
59. Feng, D.F. & Doolittle, R.F. (1996). Progressive alignment of amino acid sequences and construction of phylogenetic trees from them. *Methods Enzymol.* **266**, 368-382.
60. Park, J.T., Raychaudhuri, D., Li, H., Normark, S. & Mengin-Lecreulx, D. (1998). MppA, a periplasmic binding protein essential for import of the bacterial cell wall peptide L-alanyl-β-D-glutamyl-*meso*-diaminopimelate. *J. Bacteriol.* **180**, 1215-1223.
61. McFall, E. & Newman, E.B. (1996). Amino acids as carbon sources. In *Escherichia coli and Salmonella, Cellular and Molecular Biology*. (Neidhardt *et al.* eds), pp. 358-379, ASM Press, Washington.

Because *Chemistry & Biology* operates a 'Continuous Publication System' for Research Papers, this paper has been published via the internet before being printed. The paper can be accessed from http://biomednet.com/cbiology/cmb – for further information, see the explanation on the contents pages.